Simultaneous Expression of *ABCA4* and *GPR143* Mutations: A Complex Phenotypic Manifestation

Winston Lee,[1] Kaspar Schuerch,[1] Yajing (Angela) Xie,[1] Jana Zernant,[1] Stephen H. Tsang,[1,2] Janet R. Sparrow,[1,2] and Rando Allikmets[1,2]

[1]Department of Ophthalmology, Columbia University, New York, New York, United States
[2]Department of Pathology & Cell Biology, Columbia University, New York, New York, United States

Correspondence: Rando Allikmets, Department of Ophthalmology, Eye Research Annex Rm 202, 160 Fort Washington Avenue, New York, NY 10032, USA; rla22@cumc.columbia.edu.

Submitted: March 23, 2016
Accepted: May 22, 2016

Citation: Lee W, Schuerch K, Xie Y(A), et al. Simultaneous expression of *ABCA4* and *GPR143* mutations: a complex phenotypic manifestation. *Invest Ophthalmol Vis Sci*. 2016;57:3409–3415. DOI:10.1167/iovs.16-19621

Purpose. To describe the complex, overlapping phenotype expressed in a two generation family harboring pathogenic mutations in the *ABCA4* and *GPR143* genes.

Methods. Clinical evaluation of a two generation family included quantitative autofluorescence imaging (qAF, 488-nm excitation) using a modified confocal scanning laser ophthalmoscope equipped with an internal fluorescent reference to account for varying laser power detector sensitivity, spectral-domain optical coherence tomography, and full-field ERG testing. Complete sequencing of the *ABCA4* and *GPR143* genes was carried out in each individual.

Results. Affected individuals presented with bull's eye lesions and qAF levels above the 95% confidence interval for healthy eyes; full-field ERG revealed no generalized rod dysfunction but mild implicit time delays in cone responses. Complete sequencing of the *ABCA4* gene revealed two disease-causing mutations, p.L541P and p.G1961E; and mutational phase was confirmed in each unaffected parent. Further examination in the affected patients revealed a peripheral "mud-splattered" pattern of hypopigmented RPE after which sequencing of *GPR143* revealed a novel missense variant, p.Y157C. The *GPR143* variant segregated from the father who did not exhibit any indications of retinal disease with the exception of an abnormal near-infrared autofluorescence (NIR-AF) signal distribution in the macula.

Conclusions. An individual carrying both *ABCA4* and *GPR143* disease-causing mutations can express a complex, overlapping phenotype associated with both Stargardt disease and X-linked ocular albinism (OA1). The absence of OA1-related disease changes (with the exception of NIR-AF changes associated with melanin distribution) in the father may be indicative of mild expressivity or variable gene penetrance.

Keywords: ABCA4, GPR143, Stargardt disease, X-linked ocular albinism, heterozygous carrier, co-occurrence

Progress in next-generation sequencing (NGS) technologies has vastly improved the field of medical genetics and as a result, over 8000 genes and 15,000 phenotypes have been catalogued in the Online Mendelian Inheritance in Man (OMIM) database (in the public domain; http://www.omim.org). Likewise, increasing accessibility of gene sequencing for individual patients has provided physicians and scientists the ability to make valuable genotype–phenotype correlations. The predictive power of either targeted genetic screening or clinical examination alone, however, remains limited as the phenotypic spectrum of a given monogenic disorder varies considerably between patients, and even related individuals. Deciphering the variability of disease expression may inevitably require one to extend analyses beyond the causal effect of single genes.

The clinical spectrum of Stargardt disease (STGD1; OMIM #248200), a progressive retinal disorder, typifies the complexity of both phenotypic and genotypic heterogeneity as reported in its disease expression within and among different ethnic groups.[1–8] STGD1 is caused by mutations in the ATP-binding cassette, subfamily A (*ABCA4*) gene and is estimated to affect between 1 in 8000 and 1 in 10,000 people worldwide.[9–11] A dysfunctional ABCA4 protein results in the inadequate handling of vitamin A aldehyde in photoreceptor outer segments, thereby incurring the abundant formation of phototoxic bisretinoids of lipofuscin, including A2E.[12–14] Disc shedding and subsequent phagocytosis of the outer segments by RPE cells leads to significant lysosomal accumulations of lipofuscin, which is believed to be the cellular impetus for disease.[15] The onset of STGD1 typically begins in the first two decades of life[16]; however, disease onset within later decades has also been described from mutations, which map outside the functional regions of *ABCA4*.[17,18] Due to high carrier frequencies in the general population (~1:20),[3,18,19] its reported prevalence may be a gross underestimation as in fact, multiple affected individuals across successive generations in a single family (pseudodominant inheritance) have been described on multiple occasions.[18,20–22]

The complex phenotypes resulting from the simultaneous expression of STGD1 and other inherited retina diseases such as congenital stationary night blindness (CSNB1) and retinoblastoma have been described.[23,24] Such cases of multiple Mendelian diseases, particularly in a single organ, are scarce due perhaps to infrequent incidences; however, the 1000 Genomes Project estimates that, on average, a single individual

carries approximately 250 to 300 loss-of-function variants in annotated genes and 50 to 100 variants previously implicated in inherited disorders.[25] As such, many more cases may well exist but will likely remain unrecognized without an appropriate clinical and genetic screening repertoire. Identifying such cases by integrating knowledge of genetics, epidemiology, and comprehensive tools for clinical examination would have a significant impact on the clinical care of such patients. Furthermore, the opportunity to study such rare cases will undoubtedly provide insight into the manifestation of multiple intersecting disease pathways in the human body. Here, we describe the phenotypic manifestation of a family with two affected individuals who possess *ABCA4* mutations on both alleles while simultaneously expressing the heterozygous phenotype of X-linked ocular albinism (OA1) from a novel *GPR143* mutation.

Materials and Methods

Patients and Clinical Evaluation

Each study subject was consented before participating in the study under the institutional review board protocol #AAAI9906 approved by the institutional review board at Columbia University (New York, NY, USA). The study adhered to tenets set out in the Declaration of Helsinki. Each patient underwent a complete ophthalmic examination reviewed by a retinal physician (SHT), including slit-lamp and dilated fundus examinations. Vision was assessed by the measurement of best-corrected visual acuity (BCVA; Snellen), while further structural assessments were made using color fundus photography, autofluorescence (AF), and spectral-domain optical coherence tomography (SD-OCT).

Clinical Data Acquisition and Analysis

Spectral-domain OCT scans and corresponding fundus images were acquired using a Spectralis HRA+OCT (Heidelberg Engineering, Heidelberg, Germany). Both standard fundus autofluorescence (488-nm excitation) and near-infrared (NIR) fundus AF (787-nm excitation) were obtained using a confocal scanning-laser ophthalmoscope (Heidelberg Retina Angiograph 2, Heidelberg Engineering, Dossenheim, Germany). Fundus AF images were acquired by illuminating the fundus with an argon laser source (488 nm) and viewing the resultant fluorescence through a band pass filter with a short wavelength cut off at 495 nm. Color fundus photos were obtained with a FF 450plus Fundus Camera (Carl Zeiss Meditec AG, Jena, Germany).

Electroretinograms (ERG) in the affected siblings were recorded using the Diagnosys Espion Electrophysiology System (Diagnosys LLC, Littleton, MA, USA). For each recording, the pupils were maximally dilated and measured before full-field ERG testing using guttate tropicamide (1%) and phenylephrine hydrochloride (2.5%); and the corneas were anesthetized with guttate proparacaine 0.5%. Silver impregnated fiber electrodes (DTL; Diagnosys LLC, Littleton, MA, USA) were used with a ground electrode on the forehead. Full-field ERGs to test generalized retinal function were performed using extended testing protocols incorporating the International Society for Clinical Electrophysiology of Vision standard.[26]

Quantitative autofluorescence (qAF) was analyzed in the two affected sisters (II-2 and II-3). Protocols for the acquisition of AF images that meet the quality standards necessary for quantification have been previously described.[27,28] Fundus AF images (30°; 488-nm excitation) were acquired using a confocal scanning laser ophthalmoscope (Spectralis HRA+OCT; Heidelberg Engineering, Heidelberg, Germany) modified by the insertion of an internal fluorescent reference to account for variations in laser power and detector gain. The barrier filter in the device transmitted light from 500 to 680 nm. Prior to acquisition, the fundus is exposed to the AF light for 20 to 30 seconds to bleach rhodopsin, while at the same time, focus and alignment were refined to produce a maximum and uniform signal over the entire field.

Fundus AF images were analyzed with a dedicated image analysis software written in IGOR (WaveMetrics, Lake Oswego, OR, USA) to determine qAF. The software recorded the mean gray levels (GLs) of the internal reference and of eight circularly arranged segments positioned at an eccentricity of approximately 7° to 9° (Fig. 1E). Segments were scaled to the horizontal distance between the fovea and the temporal edge of the optic disc. Control values used in this study consisted of previously published data from 277 healthy subjects (374 eyes; age range, 5–60 years) without a family history of retinal dystrophy.[29]

Genetic Analyses

Screening of the *ABCA4* gene was performed in the affected siblings (II-2 and II-3) and detected variants were subsequently validated in the unaffected relatives for phase and carrier status by next-generation sequencing (NGS) as described before.[19] The NGS reads were analyzed and compared with the reference genome GRCh37/hg19, using the variant discovery software NextGENe (SoftGenetics LLC, State College, PA, USA). All detected possibly disease-associated variants were confirmed by Sanger sequencing segregation of the variants with the disease was analyzed in the mother and father. The allele frequencies of p.L541P and p.G1961E were compared with the ExAC database (in the public domain, http://exac.broadinstitute.org/); accessed September 2015.

Results

The proband, a 27-year-old woman, and her 24-year-old sister, presented to the clinic with macular disease, uncorrectable vision loss and a negative family history of retinal diseases. Best-corrected visual acuities were found to be 20/200 bilaterally in both siblings. Elliptical bull's eye lesions with granular hyperAF borders and fine yellow flecks (II-2, OD) were noted around the fovea on fundoscopy and AF imaging (Fig. 1A). Spectral-domain OCT scans revealed a focal loss of the ellipsoid zone band within the foveal region that is consistent with the optical gap or optically empty lesion phenotype described in STGD1[30] (Fig. 1B). Results from full-field ERG testing revealed no significantly generalized rod and cone dysfunction in the retina with the exception of mild implicit time delays in single flash cone responses in the proband and her sister (blue and red traces, respectively) when compared with the response of an age-matched healthy eye (dotted gray trace; Fig. 1C). Direct sequencing of the *ABCA4* gene in the sisters disclosed two known disease-causing mutations, p.L541P and p.G1961E, which were validated in the reportedly unaffected parents (Fig. 1D, pedigree).

Quantitative measurements of autofluorescence were obtained in the proband and her sister according to methods previously described.[27,28] Color-coded maps (Fig. 1E), scaled to qAF-units (0–1200), revealed both global and localized increases in qAF in the macula, particularly in the temporal region as compared to an age-matched healthy individual. An average qAF value taken from eight circularly arranged segments (defined as qAF_8; Fig. 1E, outlined in white) was calculated in both eyes. The inner and outer radii of the segments are scaled according to the horizontal distance

Investigative Ophthalmology & Visual Science

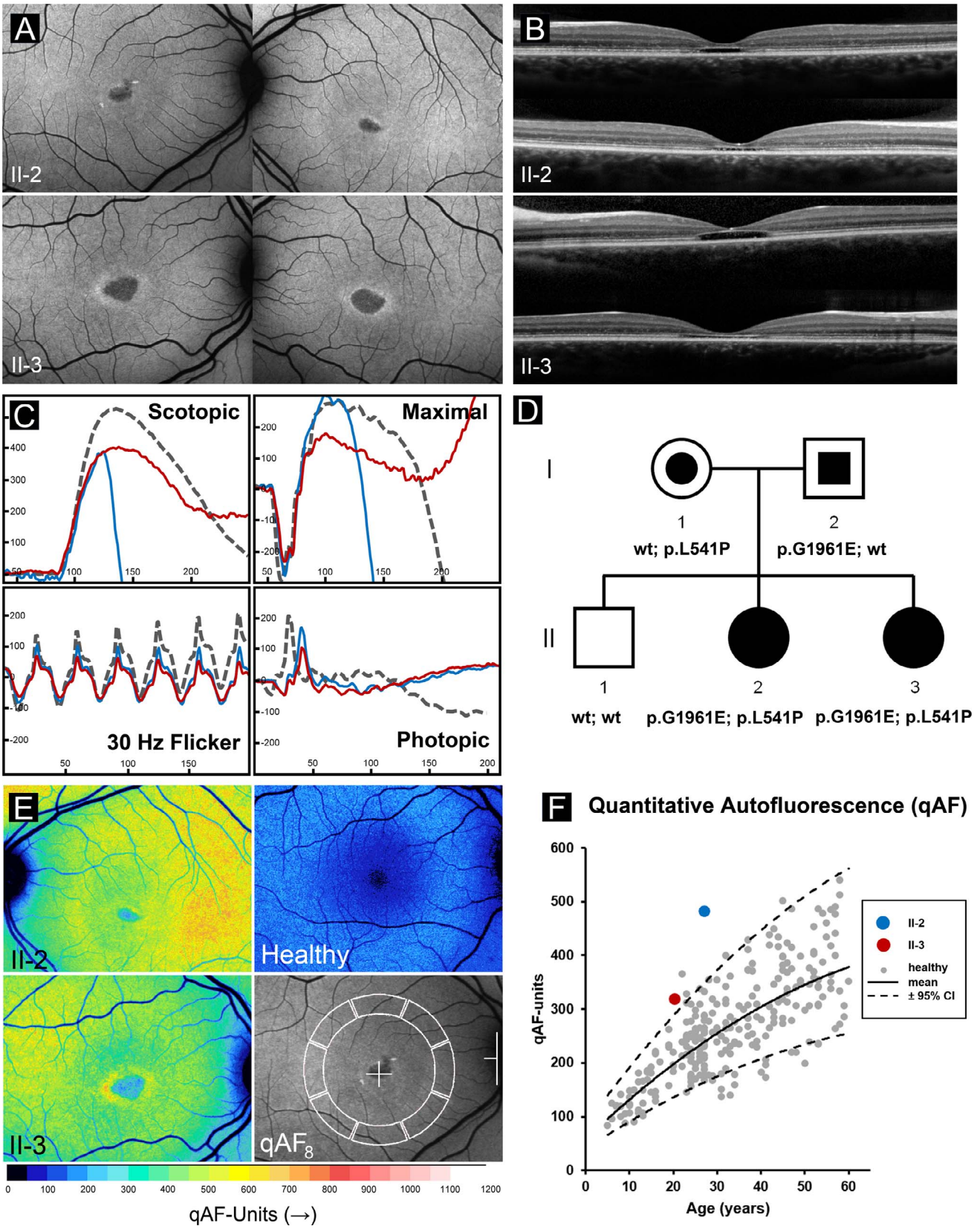

Figure 1. Clinical characterization of the proband (II-2) and affected sister (II-3) harboring the p.G1961E and p.L541P mutations of *ABCA4*. (**A**) Autofluorescence imaging revealed confined bull's eye maculopathy lesions in both eyes of the siblings corresponding to (**B**) optically empty lesion on SD-OCT. (**C**) Full-field ERG traces in II-2 (*blue*) and II-3 (*red*) showing generally preserved rod and cone function in the retina with the exception of mild implicit time delays in single flash cone responses when compared with the responses of an age-matched healthy eye. (**D**) Pedigree of the family illustrating segregation of the *ABCA4* mutations from the unaffected parents. (**E**) Color maps of quantitative autofluorescence levels (qAF-units) in II-2, II-3, and an age-matched healthy individual. Analysis of qAF was measured in eight scaled segments (qAF_8) within the macula. (**F**) Quantitative AF_8 levels in II-2 and II-3 were elevated, falling outside the 95% confidence interval of qAF_8 in healthy individuals.

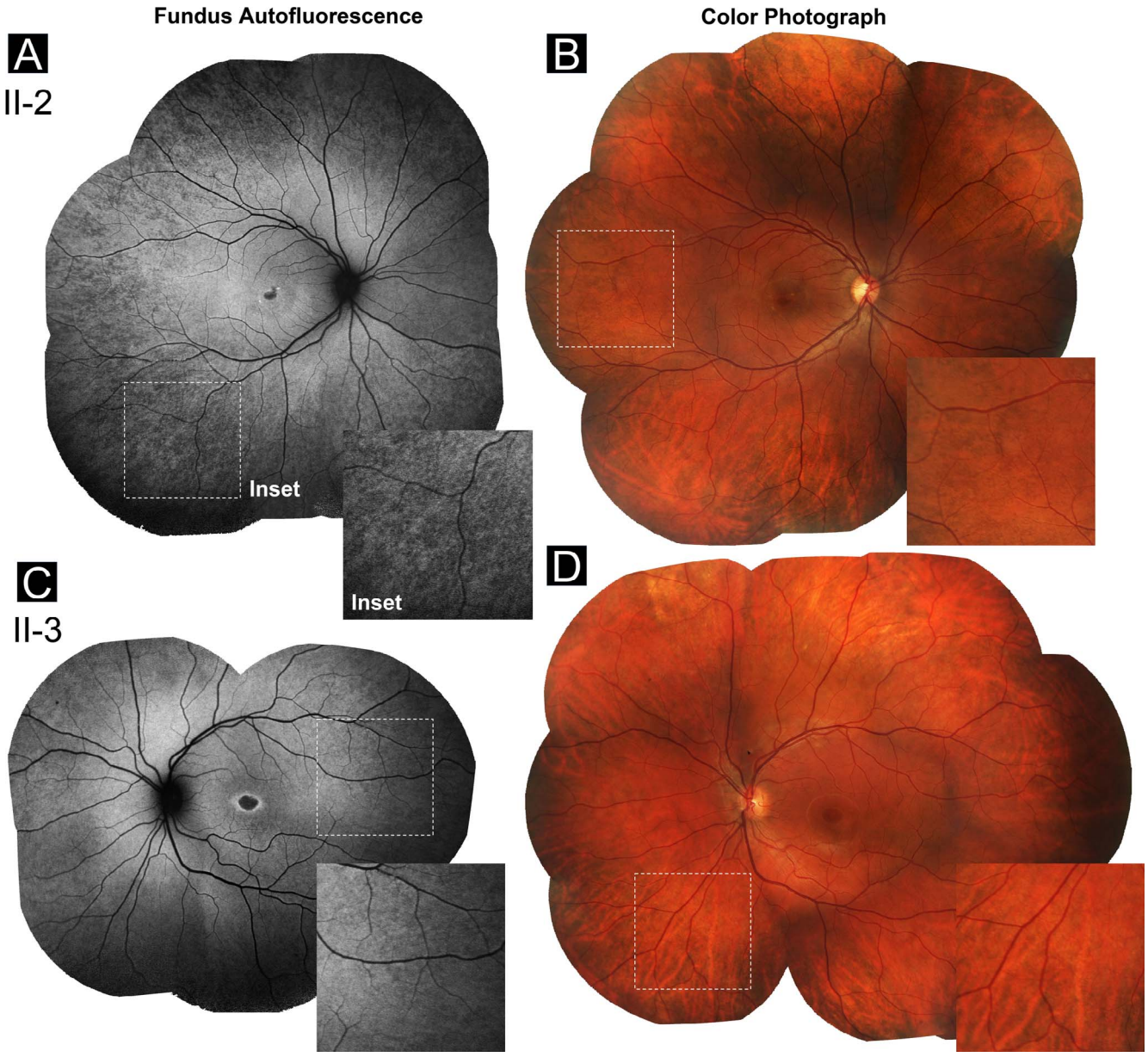

Figure 2. Wide-field montage of AF imaging and color fundus photographs in the proband (II-2) and affected sister (II-3) harboring the p.G1961E and p.L541P mutations of *ABCA4*. (**A**) A "mud-splatted" pattern of fundus hypopigmentation pattern was evident on AF and color fundus photographs in the peripheral retina in II-2 (**A**, **B**) and II-3 (**C**, **D**). The hypopigmentation pattern was notably absent in and around the macula.

between the temporal edge of the optic disc and the center of the fovea. In keeping with previously published qAF levels in STGD1,[27] qAF_8 (mean of both eyes) values in both sisters were increased (average qAF_8 OU = 466.6, proband; 320.3, sister), falling outside the 95% confidence intervals of healthy subjects when plotted as a function of age (Fig. 1F).

Fundoscopic examination of the periphery and wide-field AF imaging in the affected sisters revealed an unexpected mosaic pattern of dark patches radially distributed across the posterior pole; however, this pattern was not discernable in the macula (Figs. 2A, 2C). Corresponding areas on color images revealed a mottled, "mud-splattered" pattern of fundus hypopigmentation (Figs. 2B, 2D). Direct sequencing of the *GPR143* gene in the family uncovered an unreported missense variant, c.A470G (p.Y157C), in the affected siblings and, unexpectedly, the father (Figs. 3G, 3H) who had previously reported no history of visual symptoms. The variants' allele frequency in the population is 0.0052% and 0.03% according to the ExAC (in the public domain, http://exac.broadinstitute.org/) and ESP6500 (in the public domain, http://evs.gs.washington.edu/EVS/) databases, respectively, and its nucleotide position is moderately conserved as predicted by phyloP (phyloP: 3.92) although it is highly conserved across 11 species up to Tetraodon. The mutational change was predicted to be deleterious or damaging by all four, sorting Intolerant from Tolerant (score: 0) (SIFT; in the public domain, http://sift.jcvi.org/), Polyphen-2 (score: 1) and MutationTaster (*P* value: 1) predictive software programs.

A full examination of the other immediate relatives, parents and brother, was completely unremarkable for ocular disease. The father had BCVA of 20/15 in both eyes and multimodal retinal imaging confirmed the absence of any significant disease-related changes (Figs. 3A, 3B). Near-infrared AF (787-nm excitation) imaging of choroidal and RPE melanin showed

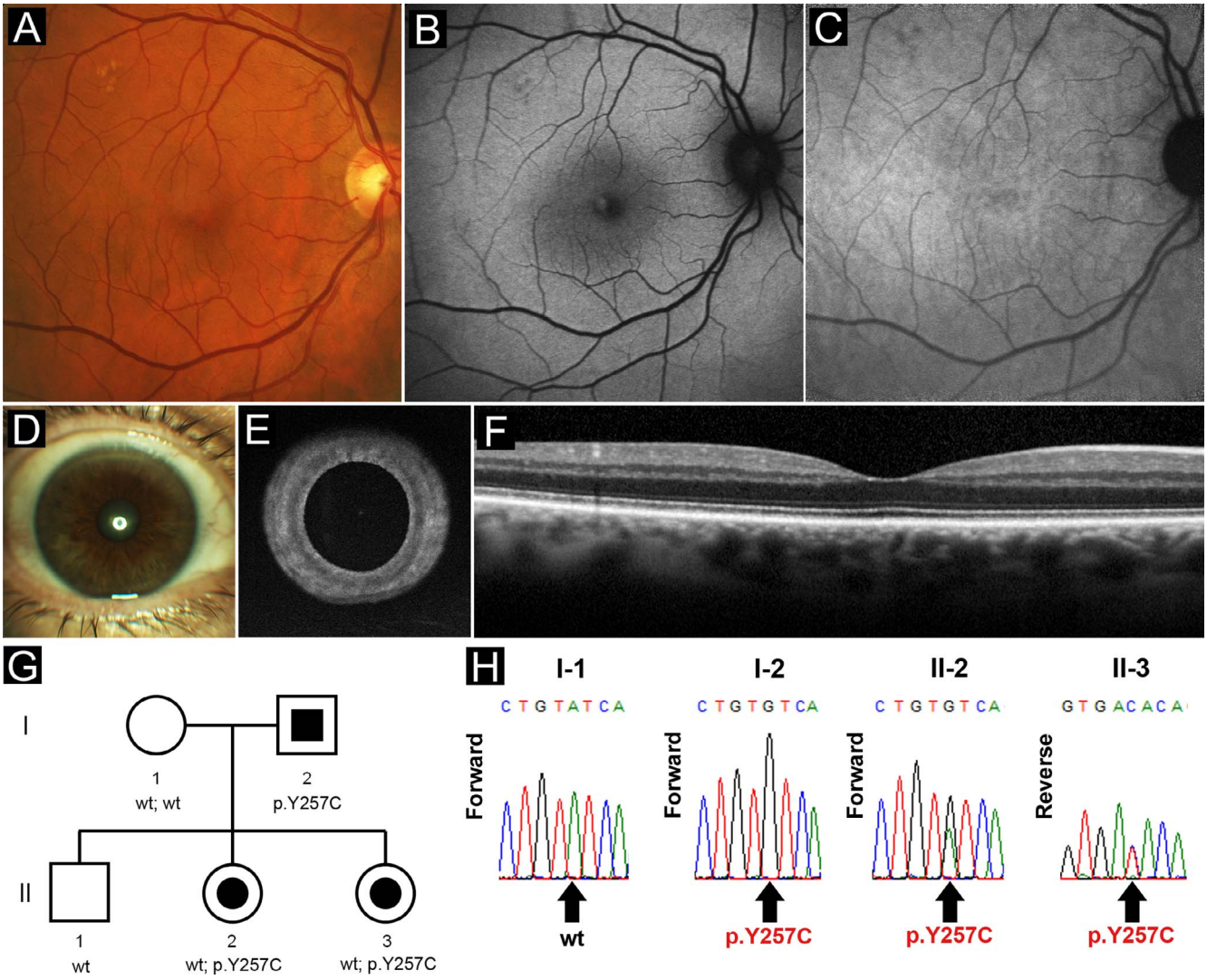

Figure 3. An absence of disease expression was confirmed in the father (I-1) of the affected proband and sister. Despite harboring the expected disease-causing p.Y257C mutation of in *GPR143*, the father exhibited no symptoms or disease changes in the macula related to X-linked ocular albinism on (**A**) color fundus photographs and (**B**) AF imaging; however, (**C**) NIR-AF (melanin) imaging revealed the absence of a high signal over the foveal region that is typically seen in healthy eyes. Iris pigmentation was normal as it appeared on a (**D**) color photograph and (**E**) NIR imaging and no signs of foveal hypoplasia was observed on (**F**) SD-OCT. (**G**) Pedigree of the family illustrating the segregation of the p.Y257C mutation of *GPR143* from the father to the siblings. (**H**) Chromatograms confirming the c.A470G (p.Y157C) peaks in father (I-1) and daughters (II-2, II-3) but not the mother (I-2).

no abnormal iris but the absence of the increased signal over the foveal region as seen in healthy eyes. (Figs. 3C–E) The presence of a normal foveal depression is apparent on SD-OCT (Fig. 3F). The father reported no family history of retinal disease particularly that which is associated with OA1.

Discussion

In addition to the two disease alleles in *ABCA4*, this family was also found to harbor a novel, likely pathogenic mutation in *GPR143* resulting in a combined STGD1 disease and heterozygous carrier phenotype in the affected sisters (II-2 and II-3). The prevalence of both Stargardt disease and OA1 are approximately 1:10,000 (with a carrier frequency of ~5%)[3,18,19] and 1:50,000,[31,32] respectively, making such an occurrence highly improbable (~1 in 500 million). Nevertheless, the subsequent finding had a significant impact on genetic counseling in the affected daughters.

Although both STGD1 and OA1 are diseases of the outer retina, it is unclear if or how both disease phenotypes would interact as the respective protein products of *ABCA4* and *GPR143* are localized to distinct cell types (photoreceptor and RPE cells, respectively). The peripheral "mud-splattered" appearance of the fundus in the affected siblings is a well-described mosaic pattern of RPE pigmentation in carrier females of *GPR143* that occurs throughout the posterior pole as a result of random x-inactivation of cells.[33–36] The pattern in both siblings, however, appears to be "masked" anteriorly by an increased distribution of AF in the macula, a disease feature consistent with ABCA4 dysfunction.[27,28,37] This apparent absence ("masking") of the underlying RPE phenotype by an increased emission of AF in the macula may be explained by several possibilities. Increased lipofuscin accumulation in the area may be displacing mislocalized melanosomes at the apical surface of RPE, thereby reducing visibility of any pigmentary characteristics. Likewise, apart from accumulated lipofuscin in subjacent RPE, a rapid increase of fluorophores residing in

photoreceptor inner and outer segment[38] may provide an additional contribution to the 488-nm signal further shielding visibility of RPE characteristics.

The reason(s) for absence of disease expression in the father, from whom the *GPR143* mutation segregated, are unclear. Disease features of *GPR143* (OA1) are of congenital onset and include nystagmus, iris translucency, macular hypoplasia, fundus hypopigmentation, and normal pigmentation of skin and hair.[39–41] Over 100 pathogenic mutations in *GPR143* have been reported of which approximately 48% are intragenic deletions while 43% are missense and splice site mutations though current methods of clinical examination have failed to identify phenotype-genotype correlations.[39] Milder OA1 phenotypes have been described; however, such cases exhibit nearly all other disease features with the exception of iris translumination and/or reduced hypopigmentation.[39,42] The absence of an increased NIR-AF signal in the foveal region described in healthy eyes may however, reveal an abnormal distribution or reduction of melanin in the father's RPE cells but it is unclear whether this finding was incidental or age-related. Such an indication of mild disease expressivity would not be unexpected as abnormalities of the fovea and RPE melanin are well-established features of OA1. The novel p.Y157C mutation reported in this family results in the substitution of a tyrosine to cysteine residue (Grantham score = 194) within the highly conserved transmembrane domain IV of the protein. The biochemical defect of this variant is unknown; however, mutations within the transmembrane domains have displayed ER retention and defective intracellular transport consistent with protein misfolding while mutations that cluster in the cytosolic loops traffic properly but are likely associated with defects in downstream signaling.[43]

Further explanations for the absence of disease expression in this single case are limited and beyond the scope of this study. Nevertheless, phenotypic variability and nonpenetrance are frequent features of monogenic diseases and much work in the last few decades has increased our understanding of genetic mosaicism and the role of epigenetics in human disease.[44,45] Hypothetically, a parental mosaicism scenario in this family would require that the *GPR143* mutation had arisen in the correct progenitor cell type and stage of embryogenesis in the father in such a way that it is exists in both somatic cells (blood leukocytes) and germline cells to be inherited by the daughters and that a small population of these cells is maintained such that the father does not or does not fully express features of OA1. Compensatory upregulation of downstream signaling may be possible, in theory, though likely insufficient for a complete phenotypic rescue given the complex role of *GPR143*. For instance, Young and colleagues[46] hypothesized and subsequently demonstrated that constitutively upregulating Gαi3, a major transducer in the murine Oa1 signaling cascade, rescues, in part, the RPE melanosomal phenotype in *Oa1*$^{-/-}$ mice.[47]

In summary, a family has been identified harboring disease-causing mutations in both *ABCA4* and *GPR143* genes resulting in a complex, overlapping disease phenotype. The affected daughters with the two *ABCA4* mutations and a single *GPR143* mutation exhibited both classical *ABCA4*-associated bull's eye maculopathy lesions and a mud-splattered hypopigmentation pattern seen in heterozygous female carriers of OA1. The hypopigmentation pattern was visible only in the periphery perhaps due to an *ABCA4*-associated elevation of lipofuscin in the macula. The *GPR143* mutation, which segregated from the father who was unexpectedly asymptomatic and exhibited no features of OA1-related changes with the exception of possible melanin-related changes seen on NIR-AF imaging, may be a disease variant associated with variable expressivity and penetrance. Co-occurring Mendelian diseases, particularly those that effect the same organ system, are rare but essential for providing valuable insight into the interactions of multiple disease pathways.

Acknowledgments

The authors thank François C. Delori of Schepens Eye Research Institute, Harvard Medical School for contributing to the development of the quantitative autofluorescence (qAF) acquisition and analysis method used in this study.

Supported, in part, by grants from the National Eye Institute/National Institutes of Health EY021163, EY019861, EY021237 and EY024091, EY019007 (Core Support for Vision Research; Bethesda, MD, USA); and unrestricted funds from Research to Prevent Blindness (New York, NY, USA) to the Department of Ophthalmology, Columbia University.

Disclosure: **W. Lee**, None; **K. Schuerch**, None; **Y.(A.) Xie**, None; **J. Zernant**, None; **S.H. Tsang**, None; **J.R. Sparrow**, None; **R. Allikmets**, None

References

1. Chacon-Camacho OF, Granillo-Alvarez M, Ayala-Ramirez R, Zenteno JC. ABCA4 mutational spectrum in Mexican patients with Stargardt disease: identification of 12 novel mutations and evidence of a founder effect for the common p.A1773V mutation. *Exp Eye Res*. 2013;109:77–82.
2. Maugeri A, Klevering BJ, Rohrschneider K, et al. Mutations in the ABCA4 (ABCR) gene are the major cause of autosomal recessive cone-rod dystrophy. *Am J Hum Genet*. 2000;67:960–966.
3. Maugeri A, van Driel MA, van de Pol DJ, et al. The 2588G→C mutation in the ABCR gene is a mild frequent founder mutation in the Western European population and allows the classification of ABCR mutations in patients with Stargardt disease. *Am J Hum Genet*. 1999;64:1024–1035.
4. Rivera A, White K, Stohr H, et al. A comprehensive survey of sequence variation in the ABCA4 (ABCR) gene in Stargardt disease and age-related macular degeneration. *Am J Hum Genet*. 2000;67:800–813.
5. Rosenberg T, Klie F, Garred P, Schwartz M. N965S is a common ABCA4 variant in Stargardt-related retinopathies in the Danish population. *Mol Vis*. 2007;13:1962–1969.
6. Sciezynska A, Ozieblo D, Ambroziak AM, et al. Next-generation sequencing of ABCA4: high frequency of complex alleles and novel mutations in patients with retinal dystrophies from Central Europe. *Exp Eye Res*. 2015;145:93–99.
7. Valverde D, Riveiro-Alvarez R, Bernal S, et al. Microarray-based mutation analysis of the ABCA4 gene in Spanish patients with Stargardt disease: evidence of a prevalent mutated allele. *Mol Vis*. 2006;12:902–908.
8. Zernant J, Collison FT, Lee W, et al. Genetic and clinical analysis of ABCA4-associated disease in African American patients. *Hum Matat*. 2014;35:1187–1194.
9. Allikmets R, Singh N, Sun H, et al. A photoreceptor cell-specific ATP-binding transporter gene (ABCR) is mutated in recessive Stargardt macular dystrophy. *Nat Genet*. 1997;15:236–246.
10. Michaelides M, Hunt DM, Moore AT. The genetics of inherited macular dystrophies. *J Med Genet*. 2003;40:641–650.
11. Blacharski P. *Fundus Flavimaculatus*. New York: Raven Press; 1988.
12. Quazi F, Lenevich S, Molday RS. ABCA4 is an N-retinylidene-phosphatidylethanolamine and phosphatidylethanolamine importer. *Nat Commun*. 2012;3:925.
13. Sparrow JR, Gregory-Roberts E, Yamamoto K, et al. The bisretinoids of retinal pigment epithelium. *Prog Retin Eye Res*. 2012;31:121–135.

14. Sun H, Smallwood PM, Nathans J. Biochemical defects in ABCR protein variants associated with human retinopathies. *Nat Genet*. 2000;26:242–246.
15. Cideciyan AV, Aleman TS, Swider M, et al. Mutations in ABCA4 result in accumulation of lipofuscin before slowing of the retinoid cycle: a reappraisal of the human disease sequence. *Hum Mol Genet*. 2004;13:525–534.
16. Weleber RG. Stargardt's macular dystrophy. *Arch Ophthalmol*. 1994;112:752–754.
17. Westeneng-van Haaften SC, Boon CJ, Cremers FP, Hoefsloot LH, den Hollander AI, Hoyng CB. Clinical and genetic characteristics of late-onset Stargardt's disease. *Ophthalmology*. 2012;119:1199–1210.
18. Yatsenko AN, Shroyer NF, Lewis RA, Lupski JR. Late-onset Stargardt disease is associated with missense mutations that map outside known functional regions of ABCR (ABCA4). *Hum Genet*. 2001;108:346–355.
19. Zernant J, Schubert C, Im KM, et al. Analysis of the ABCA4 gene by next-generation sequencing. *Invest Ophthalmol Vis Sci*. 2011;52:8479–8487.
20. Lee W, Xie Y, Zernant J, et al. Complex inheritance of ABCA4 disease: four mutations in a family with multiple macular phenotypes. *Hum Genet*. 2016;135:9–19.
21. Cremers FP, van de Pol DJ, van Driel M, et al. Autosomal recessive retinitis pigmentosa and cone-rod dystrophy caused by splice site mutations in the Stargardt's disease gene ABCR. *Hum Mol Genet*. 1998;7:355–362.
22. Lewis RA, Shroyer NF, Singh N, et al. Genotype/phenotype analysis of a photoreceptor-specific ATP-binding cassette transporter gene, ABCR, in Stargardt disease. *Am J Hum Genet*. 1999;64:422–434.
23. Huynh N, Jeffrey BG, Turriff A, Sieving PA, Cukras CA. Sorting out co-occurrence of rare monogenic retinopathies: Stargardt disease co-existing with congenital stationary night blindness. *Ophthalmic Genet*. 2014;35:51–56.
24. Margalit E, Sunness JS, Green WR, et al. Stargardt disease in a patient with retinoblastoma. *Arch Ophthalmol*. 2003;121:1643–1646.
25. Genomes Project C, Abecasis GR, Altshuler D, et al. A map of human genome variation from population-scale sequencing. *Nature*. 2010;467:1061–1073.
26. McCulloch DL, Marmor MF, Brigell MG, et al. ISCEV Standard for full-field clinical electroretinography (2015 update). *Doc Ophthalmol*. 2015;130:1–12.
27. Burke TR, Duncker T, Woods RL, et al. Quantitative fundus autofluorescence in recessive Stargardt disease. *Invest Ophthalmol Vis Sci*. 2014;55:2841–2852.
28. Delori F, Greenberg JP, Woods RL, et al. Quantitative measurements of autofluorescence with the scanning laser ophthalmoscope. *Invest Ophthalmol Vis Sci*. 2011;52:9379–9390.
29. Greenberg JP, Duncker T, Woods RL, Smith RT, Sparrow JR, Delori FC. Quantitative fundus autofluorescence in healthy eyes. *Invest Ophthalmol Vis Sci*. 2013;54:5684–5693.
30. Noupuu K, Lee W, Zernant J, Tsang SH, Allikmets R. Structural and genetic assessment of the ABCA4-associated optical gap phenotype. *Invest Ophthalmol Vis Sci*. 2014;55:7217–7226.
31. Incerti B, Cortese K, Pizzigoni A, et al. Oa1 knock-out: new insights on the pathogenesis of ocular albinism type 1. *Hum Mol Genet*. 2000;9:2781–2788.
32. Oetting WS. New insights into ocular albinism type 1 (OA1): mutations and polymorphisms of the OA1 gene. *Hum Matat*. 2002;19:85–92.
33. Charles SJ, Moore AT, Grant JW, Yates JR. Genetic counselling in X-linked ocular albinism: clinical features of the carrier state. *Eye*. 1992;6(Pt 1):75–79.
34. Falls HF. Sex-linked ocular albinism displaying typical fundus changes in the female heterozygote. *Am J Ophthalmol*. 1951;34:41–50.
35. Lyon MF. Sex chromatin and gene action in the mammalian X-chromosome. *Am J Hum Genet*. 1962;14:135–148.
36. Moshiri A, Scholl HP, Canto-Soler MV, Goldberg MF. Morphogenetic model for radial streaking in the fundus of the carrier state of X-linked albinism. *JAMA Ophthalmol*. 2013;131:691–693.
37. Duncker T, Tsang SH, Lee W, et al. Quantitative fundus autofluorescence distinguishes ABCA4-associated and non-ABCA4-associated bull's-eye maculopathy. *Ophthalmology*. 2015;122:345–355.
38. Birnbach CD, Jarvelainen M, Possin DE, Milam AH. Histopathology and immunocytochemistry of the neurosensory retina in fundus flavimaculatus. *Ophthalmology*. 1994;101:1211–1219.
39. Rosenberg T, Schwartz M. X-linked ocular albinism: prevalence and mutations–a national study. *Eur J Hum Genet*. 1998;6:570–577.
40. Schnur RE, Wick PA, Bailey C, et al. Phenotypic variability in X-linked ocular albinism: relationship to linkage genotypes. *Am J Hum Genet*. 1994;55:484–496.
41. Xiao X, Zhang Q. Iris hyperpigmentation in a Chinese family with ocular albinism and the GPR143 mutation. *Am J Med Genet Part A*. 2009;149A:1786–1788.
42. Pan Q, Yi C, Xu T, et al. A novel mutation, c.494C>A (p.Ala165Asp), in the GPR143 gene causes a mild phenotype in a Chinese X-linked ocular albinism patient. *Acta Ophthalmol*. 2015;94:417–418.
43. d'Addio M, Pizzigoni A, Bassi MT, et al. Defective intracellular transport and processing of OA1 is a major cause of ocular albinism type 1. *Hum Mol Genet*. 2000;9:3011–3018.
44. Biesecker LG, Spinner NB. A genomic view of mosaicism and human disease. *Nat Rev Genet*. 2013;14:307–320.
45. Genin E, Feingold J, Clerget-Darpoux F. Identifying modifier genes of monogenic disease: strategies and difficulties. *Hum Genet*. 2008;124:357–368.
46. Young A, Powelson EB, Whitney IE, et al. Involvement of OA1, an intracellular GPCR, and G alpha i3, its binding protein, in melanosomal biogenesis and optic pathway formation. *Invest Ophthalmol Vis Sci*. 2008;49:3245–3252.
47. Young A, Wang Y, Ahmedli NB, Jiang M, Farber DB. A constitutively active Galphai3 protein corrects the abnormal retinal pigment epithelium phenotype of Oa1–/– mice. *PLoS One*. 2013;8:e76240.

Investigative Ophthalmology & Visual Science